Near-infrared transillumination guides administration of dental 2D radiography and CBCT imaging

Keith Angelino
Media Lab
Massachusetts Institute of Technology
Cambridge, MA United States
kla11@media.mit.edu

David Edlund
Hampden Dental Care
Lakewood, CO United States
davidedlund777@gmail.com

Gaurav Bhatia
Media Lab
Massachusetts Institute of Technology
Cambridge, MA United States
ggbhatia@media.mit.edu

Sharon Wu
Media Lab
Massachusetts Institute of Technology
Cambridge, MA United States
sharonwu@mit.edu

Pratik Shah*
Media Lab
Massachusetts Institute of Technology
Cambridge, MA United States
pratiks@media.mit.edu
* Corresponding author.

***Abstract*—Cone beam computed tomography (CBCT) can provide enhanced information for diagnosing dental diseases when compared to 2D radiographs. However, other non-ionizing imaging modes such as near-infrared transillumination may have clinical potential to supplement radiographic methods. In a study of 13 extracted human teeth, we compared clinical features between 2D radiograph, CBCT, and near-infrared transillumination imaging. We found that near-infrared imaging independently, and in some cases exclusively, was successful in identifying early demineralization and shallow enamel features, while radiography was optimal for capturing deeper decay and developed caries. We report that near-infrared transillumination imaging is well-suited for rapid screening of patients for detection of early problem sites and as a preliminary assessment tool to guide administration of radiographs.**

Keywords-caries; CBCT; demineralization; dental imaging; near-infrared; radiography

I. INTRODUCTION

The near-infrared (NIR) spectrum is of particular biomedical significance as NIR light penetrates more deeply into tissue than visible light [1]. However, longer NIR wavelengths are increasingly absorbed by water and other common bodily constituents, leading to a narrow wavelength range known informally to biomedical researchers as the "NIR/optical/therapeutic window". This window spans most of the NIR spectrum and is the principle behind various medical research fields, most notably in methods such as NIR spectroscopy, fluorescence imaging, and optical coherence tomography [2]. Furthermore, NIR light is non-ionizing and commonly employed with non-destructive detection systems, supporting its use for *in vivo* and *in vitro* applications.

The use of NIR light for dental imaging remains an active area of research. While tooth enamel is the hardest and most mineralized tissue in the human body [3, 4], it is translucent in the near-infrared range [5-8]; refer to Fig. 1a for a generalized anatomy of the tooth. Dentin is also translucent under NIR illumination, but to a lesser extent due to its greater scattering properties [9], organizational structure [10], and high water content [5]. Tooth transillumination is a popular method for NIR dental imaging [5-8, 10-23], where the NIR source is placed on one side of the tooth, typically close to or directly adjacent to a surface; the camera sensor is then positioned orthogonal to, or on the opposite side of, the tooth. Enamel transparency improves with increasing wavelength up to approximately 1310 nm [13, 14, 24]; however, dental caries and demineralized regions scatter NIR light and appear as dark areas [5, 14, 25]. The extent of the caries can be assessed by comparing the dark and translucent areas at different viewing angles. Evaluated against 2D radiographs, NIR imaging has been shown to capture a higher level of detail of demineralized and carious enamel [11, 13]. Previous work from our group has reported the utility of NIR point-of-care devices for the recognition of enamel features that may not yet appear on a 2D radiograph, granting the clinician an earlier chance to prescribe corrective action [26].

2471-7819/17/31.00 ©2017 IEEE
DOI 10.1109/BIBE.2017.00062

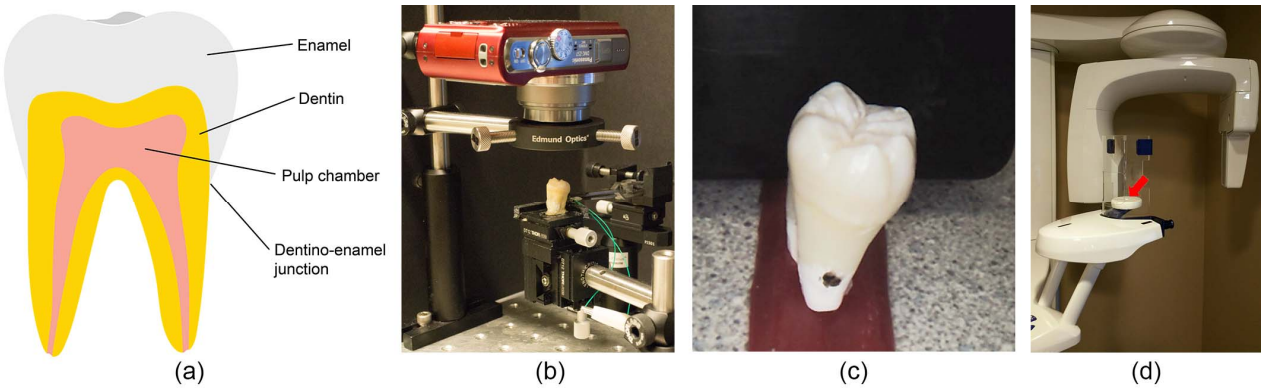

Figure 1. (a) Generalized tooth structure. (b) NIR transillumination: tooth is placed in front of a camera and transilluminated by an 850 nm LED. In this view, the tooth was imaged occlusally, with the LED directed orthogonal to the viewing plane (as pictured here); teeth can also be imaged in an inline transillumination orientation, where the tooth is placed directly between the camera and LED (not pictured). (c) 2D radiographic: tooth placed in front of the X-ray sensor, with X-rays directed into the surface marked with the dot. The dot will not appear on the radiograph. (d) CBCT: tooth is positioned between the rotating arms, as marked by the arrow.

While conventional X-ray machines can rapidly image entire sections of the mouth and allow for qualitative assessment of the maxillary and mandibular jawbone, the increasing prominence of 3D digital radiography, such as with cone beam computed tomography (CBCT), has significantly enhanced diagnostic capability and treatment. The digitally-reconstructed CBCT models of the oral cavity can be sectioned in any orientation to find and closely assess disease. As such, CBCT imaging can provide higher specificity in identifying the extent of carious lesions over 2D radiographs. Furthermore, the models are resolute enough for application to various dental specialties, such as endodontic root assessment, prosthodontics, or for use in surgery. However, similar to 2D radiography, CBCT imaging has generated concern among patients who seek to reduce their exposure to ionizing radiation [27]. It is not uncommon for patients to refuse radiographs, and dentists who lack radiographs of a patient are denied valuable diagnostic information. As an emerging technology, CBCT machines also carry a high cost and are of low availability.

In this report, we examine and compare features in multiple extracted teeth using conventional radiographic, CBCT imaging, and NIR transillumination modes. We establish that NIR imaging can provide unique diagnostic value, primarily in its ability to reveal the extent of surface demineralization. We also provide examples where NIR illumination indicated underlying problem sites in need of further clinical attention and propose the use of NIR imaging to guide targeted and rational use of ionizing radiation in patients.

II. Methods

A. Sample preparation

Thirteen extracted molars and premolars were obtained during routine dental procedures from multiple individuals who provided consent for NIR imaging (MIT IRB No. 1603518840). No personal or medical details of the individuals were recorded. While in storage, teeth were immersed in a 2% sodium hypochlorite solution and refrigerated. Teeth were allowed to air dry prior to image capture.

B. NIR imaging

NIR imaging was achieved with a Panasonic Lumix DMC-ZS7 (Panasonic Corporation, Osaka, Japan) camera modified to have its infrared filter removed, which granted the CCD sensor access to a portion of the NIR spectrum. The camera was mounted to an optical bench inline to a translation stage (Fig. 1b). To block visible light, a FGL780 longpass filter (Thorlabs, Inc., New Jersey, USA) with a cut-on of 780 nm was positioned directly in front of the camera lens, with seams between the filter and lens optically shielded. The filter has an approximate 90% transmission rate for 850 nm light. A NIR LED with a peak wavelength of 850 nm was selected for the NIR imaging. Transillumination of select NIR LEDs on extracted teeth indicated 850 nm as the most ideal for use with the camera.

Image capture was performed by mounting a tooth of interest upright on the stage, with the 850 nm LED positioned directly adjacent to the root. The Panasonic camera was then oriented downward to image the occlusal surface, or from the side to capture a facial surface. Each tooth was additionally imaged on the same stage under 1310 nm illumination with a NoblePeak Vision TriWave InGaAs infrared camera (NoblePeak Vision Corporation, Wakefield, Massachusetts, USA). This longer wavelength was used to verify the demineralized and carious lesions in the 850 nm images as non-pigmentation.

C. White light

A white light image of each tooth was obtained with a Canon EOS M digital camera (Canon Inc., Ōta, Tokyo). The same stage from the NIR imaging setup was used for mounting the teeth during photography.

D. Radiography

For 2D radiographs, a Kodak RVG 6100 Digital Radiography System (Carestream Dental, Atlanta, GA) was

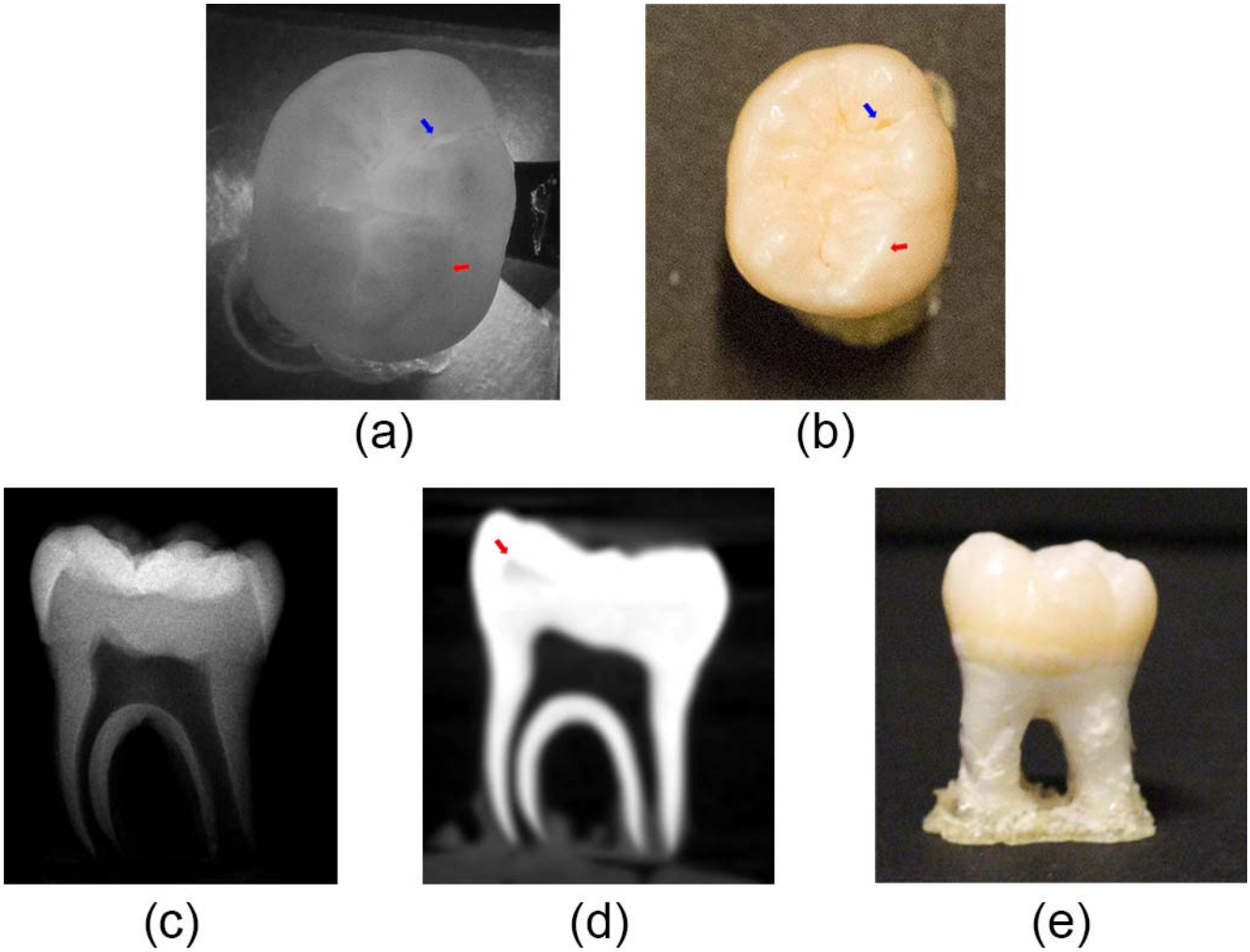

Figure 2. Images of extracted tooth sample 1. (a) NIR occlusal transillumination; (b) white light occlusal; (c) 2D radiograph; (d) CBCT radiographic slice; (e) white light. All of the whiter regions on the occlusal surface in (e) are specular reflection and not white spots or demineralization, including those marked by the red arrow.

used to image teeth in a standard bitewing orientation (Fig. 1c). Samples were placed on a wax pad and positioned in a bitewing orientation. An X-ray sensor was positioned behind the tooth, and the X-ray source aimed directly at the tooth and orthogonal to the sensor.

For CBCT imaging, each extracted tooth was positioned in a Planmeca ProMax 3D Max imaging system (Planmeca, Helsinki, Finland) (Fig. 1d). A full radiographic scan of each tooth was performed, and both the radiographic data and digitally-reconstructed 3D model were analyzed in the Planmeca Romexis software suite. The minimum resolution of the CBCT machine was 160 µm, which delineates approximate feature and tomographic slice sizes.

III. Results and Discussion

Fig. 2 shows a molar exhibiting a large patch of demineralization visible under NIR occlusal transillumination (Fig. 2a, red arrow). The demineralization was not apparent in the occlusal white light image (Fig. 2b, red arrow) or to the dentist; any white regions in Fig. 2b are the result of specular reflection. While the 2D radiograph (Fig. 2c) provided poor evidence of this demineralized area, the CBCT radiographic slice displayed caries forming under the dentino-enamel junction (Fig. 2d, red arrow) with a position corresponding to the site of demineralization in Fig. 2a. Furthermore, a sizable pit was a suspected site of penetrated enamel during visual examination (Fig. 2b, blue arrow); however, this pit contained no visible demineralization under NIR imaging (Fig. 2a, blue arrow) and no corresponding radiographic evidence of underlying lesions, demonstrating the value of preliminary NIR surface imaging when triaging false positives.

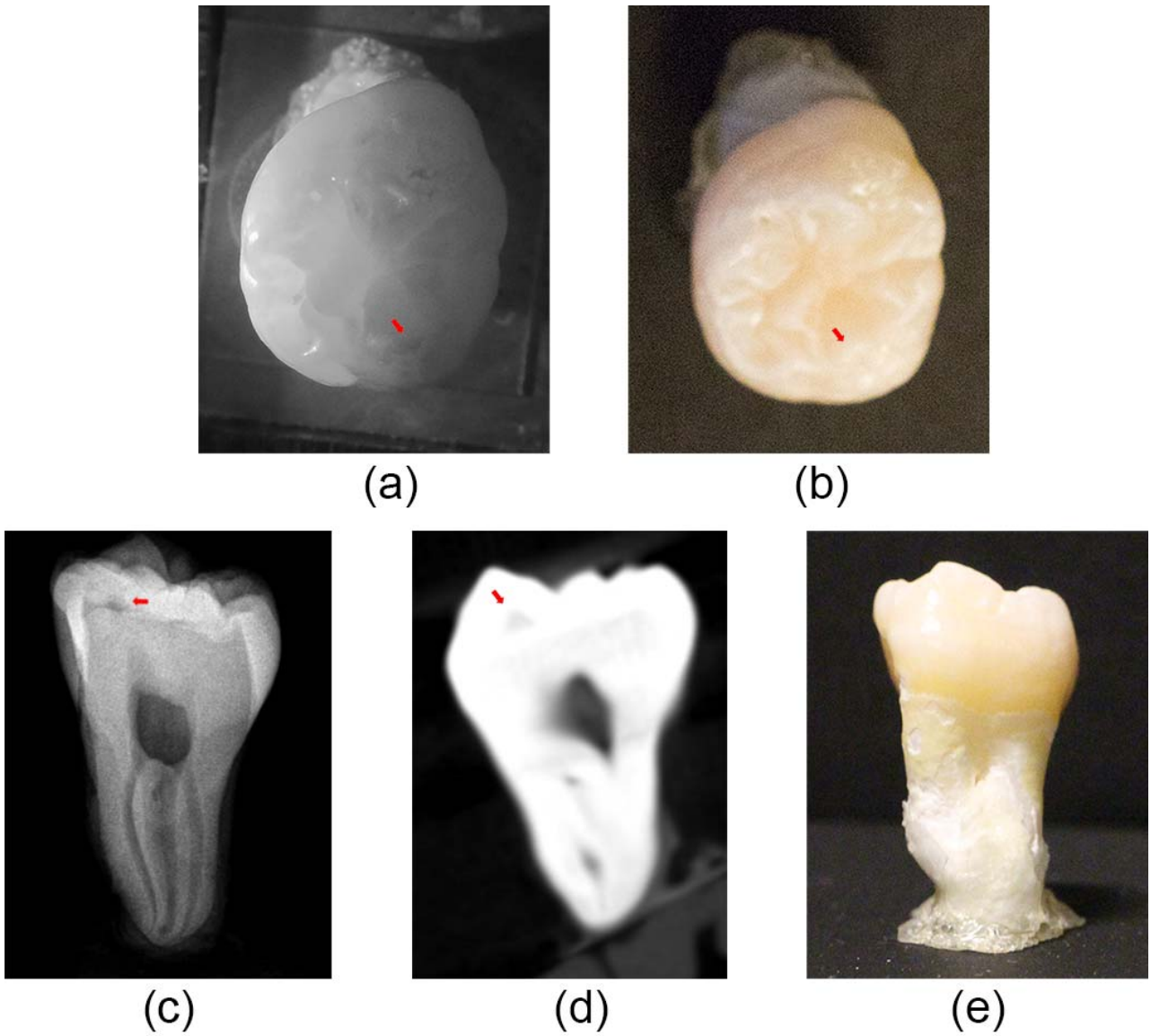

Figure 3. Images of extracted tooth sample 2. (a) NIR occlusal transillumination; (b) white light occlusal; (c) 2D radiograph; (d) CBCT radiographic slice; (e) white light.

In the tooth in Fig. 3, close examination of a dark region under NIR occlusal transillumination imaging allowed for the identification of an entry point (Fig. 3a, red arrow) for the caries seen at the dentino-enamel junction in both the 2D radiograph (Fig. 3c, red arrow) and CBCT slice (Fig. 3d, red arrow). This same region contained no pigmentation and showed no surface white spots in visible light (Fig. 3b, red arrow), and otherwise appeared intact and healthy.

The tooth in Fig. 4 exhibits heavy occlusal demineralization. The fissures at the darkest regions appearing under NIR occlusal transillumination were identified as potential entry points for caries (Fig. 4a, red arrow). Caries was confirmed under the dentino-enamel junction by radiography; the radiolucency was less discernable in the 2D radiograph (Fig. 4e, red arrow) than the CBCT tomographic slice (Fig. 4f, red arrow). The caries was also severe enough to manifest as voids marked in the CBCT reconstruction (Fig. 4g, red arrow). Heavier staining in the occlusal white light image (Fig. 4b) at this same region is present; demineralization and no stains were present in the NIR occlusal image (Fig. 4a), which was verified by further imaging performed at 1310 nm (data not shown) [28]. Also of significance was the proximal caries marked by the blue arrows in Fig. 4d and 4e, which was much more apparent in the 2D radiograph and NIR image than it was via CBCT imaging.

Table 1 lists generalized key dental features discernible by imaging modalities. NIR imaging was preferred when revealing features on the enamel surface, immediately under the surface, and harder to see in visible light. The most pertinent examples of NIR surface utility was the exoneration of a suspect surface feature (Fig. 2a and 2b, blue arrows) and the implication of caries (Fig. 3a, red arrow) at an otherwise unremarkable region in visible light.

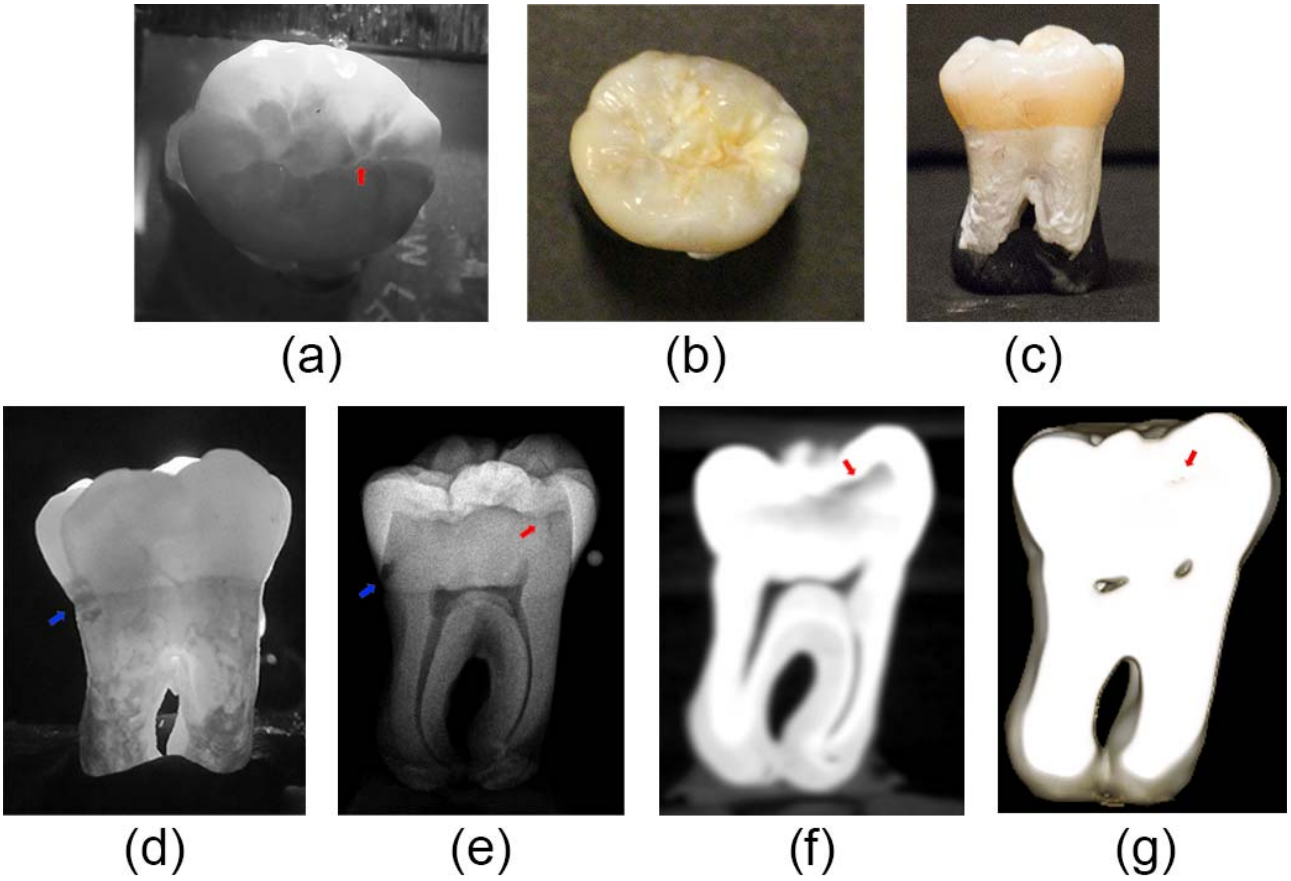

Figure 4. Images of extracted tooth sample 3. (a) NIR occlusal transillumination; (b) white light occlusal; (c) white light; (d) NIR transillumination; (e) 2D radiograph; (f) CBCT radiographic slice; (g) CBCT 3D reconstruction.

Radiographic methods excelled at subsurface analysis. 2D radiographs generally provided higher resolution single-shot images, but CBCT radiographs offered the capability to see the extent of caries through the volume of the tooth. This was easier to conceptualize when examining the tooth in the Romexis software and viewing the tomographic slices in sequence. In the same manner, NIR interrogation revealed more qualitative detail on-site by manipulating the source light and camera angle, which cannot be represented in a single image, and white light images are marred by specular reflection that is easier to disregard *in situ*.

Metal amalgam fillings directly interfered with both the tomographic slices and the 3D reconstruction of the model due to the scatter of the X-rays. The CBCT radiographs displayed lighting artifacts around the metal regions; in the 3D reconstruction, the scatter manifests as rough striations propagating off of the model. This potentially interferes with identification and assessment of secondary caries. While scattering noise in 2D radiographs is not present, the radiopaque metal obscures superimposed material. Though metal amalgam remains opaque in NIR, the margin between the filling and residual tooth can be situationally examined with a modular NIR system, as demonstrated in our prior work [26].

Also of note was that during the preliminary wavelength comparison test, it was noticed that demineralization and caries were significantly reduced in appearance at wavelengths of 1450 nm, and essentially invisible at wavelengths 1550 nm and 1650 nm. While literature has noted that enamel transparency continues to increase along with wavelength throughout the NIR range, there may not be an established upper limit to the functional imaging of demineralization, caries, and other dental features in the higher NIR and short-wavelength infrared range. Loss of contrast between caries and sound enamel at higher NIR wavelengths has been previously researched and primarily attributed to water absorption [15, 16] and secondly dentin [10], with recommendations of using reflectance NIR imaging over transillumination for better contrast. However, the disappearance of carious or demineralization regions could be potentially exploited in situations where imaging past certain features is desired.

Overall, the effectiveness of each imaging mode is highly dependent on a number of conditions outside of control including dental geography, viewing angle, and extent of disease. NIR imaging is best suited as an initial screening tool to assess the prevalence and scale of demineralization, especially on the enamel surface and at suspicious darker sites. Used in conjunction with white light examination, NIR

TABLE I. COMPARISON OF COMMON DENTAL FEATURES BETWEEN WHITE LIGHT, RADIOGRAPHIC, AND NEAR-INRAFRARED IMAGING MODES

Imaging mode	**Dental Feature**						
	White spots	*Early demineralization*	*Heavy demineralization*	*Enamel caries*	*Dentin caries*	*Mild cracks*	*Severe cracks*
Visual examination	Appears as hypomineralization / white spots	Does not appear	Appears as hypomineralization / white spots	Appears only when voids or pigmentation are present	Does not appear unless severe	Apparent	Apparent
NIR imaging	Appears as dark spots	Appears as darker regions	Appears as very dark regions	Appears as darker regions	Does not appear	Apparent	Apparent
2D radiograph	Does not appear	Does not appear	Appears as faint radiolucencies / shadows	Appears as radiolucencies /shadows	Appears as radiolucencies /shadows	Does not appear	Appears as radiolucencies
CBCT	Does not appear	Does not appear	Appears as faint radiolucencies / shadows	Appears as radiolucencies /shadows	Appears as radiolucencies /shadows	Does not appear	Appears as radiolucencies

imaging may direct implementation of localized 2D radiographs, or recommend when a full CBCT scan is required. Alternatively, radiography can follow when NIR imaging is first administered but is inconclusive. This method is also recommended from a safety perspective, as an initial NIR scan of the teeth is not harmful, while 2D radiographs and CBCT imaging use increasing amounts of ionizing radiation.

REFERENCES

[1] A. M. Smith, M. C. Mancini, and S. Nie, "Bioimaging: Second window for in vivo imaging," *Nat Nano,* vol. 4, no. 11, pp. 710-711, 2009.

[2] C. Boudoux, *Fundamentals of Biomedical Optics*, 1 ed. BLURB Incorporated, 2017, p. 448.

[3] R. Ramakrishnaiah *et al.*, "Applications of Raman Spectroscopy in Dentistry: Analysis of Tooth Structure," *Applied Spectroscopy Reviews,* vol. 50, no. 4, pp. 332-350, 2015.

[4] L. Choo-Smith, M. Hewko, and M. G. Sowa, "Emerging Dental Applications of Raman Spectroscopy," in *Emerging Raman Applications and Techniques in Biomedical and Pharmaceutical Fields*, P. Matousek and M. Morris, Eds. 1 ed. (Biological and Medical Physics, Biomedical Engineering: Springer-Verlag Berlin Heidelberg, 2010.

[5] S. Chung, D. Fried, M. Staninec, and C. L. Darling, "Multispectral near-IR reflectance and transillumination imaging of teeth," *Biomed Opt Express,* vol. 2, no. 10, pp. 2804-2814, Oct. 2011.

[6] W. A. Fried *et al.*, "Near-IR imaging of cracks in teeth," *Proc SPIE,* vol. 8929, p. 89290Q, Feb. 2014.

[7] G. C. Jones, R. S. Jones, and D. Fried, "Transillumination of interproximal caries lesions with 830-nm light," *Proc SPIE,* vol. 5313, pp. 17-22, May 2004.

[8] J. C. Simon *et al.*, "Transillumination and reflectance probes for in vivo near-IR imaging of dental caries," *Proc SPIE,* vol. 8929, p. 89290D, Feb. 2014.

[9] C. M. Bühler, P. Ngaotheppitak, and D. Fried, "Imaging of occlusal dental caries (decay) with near-IR light at 1310-nm," *Opt Express,* vol. 13, no. 2, pp. 573-582, Jan. 2005.

[10] A. C. Chan, C. L. Darling, K. H. Chan, and D. Fried, "Attenuation of near-IR light through dentin at wavelengths from 1300–1650-nm," *Proc SPIE,* vol. 8929, p. 89290M, 2014.

[11] A. M. A. Maia, L. Karlsson, W. Margulis, and A. S. L. Gomes, "Evaluation of two imaging techniques: near-infrared transillumination and dental radiographs for the detection of early approximal enamel caries," *Dentomaxillofacial Radiol,* vol. 40, no. 7, pp. 429-433, Oct. 2011.

[12] J. Kühnisch *et al.*, "In vivo validation of near-infrared light transillumination for interproximal dentin caries detection," *Clin Oral Investig,* vol. 20, no. 4, pp. 821-829, May 2016.

[13] R. S. Jones, G. D. Huynh, G. C. Jones, and D. Fried, "Near-infrared transillumination at 1310-nm for the imaging of early dental decay," *Optics Express,* vol. 11, no. 18, pp. 2259-2265, Sept. 2003.

[14] C. L. Darling, G. D. Huynh, and D. Fried, "Light scattering properties of natural and artificially demineralized dental enamel at 1310nm," *J Biomed Opt,* vol. 11, no. 3, pp. 34011-34023, May 2006.

[15] J. C. Simon *et al.*, "Near-IR transillumination and reflectance imaging at 1,300 nm and 1,500–1,700 nm for in vivo caries detection," *Lasers in Surgery and Med,* vol. 48, no. 9, pp. 828-836, Jul. 2016.

[16] S. Chung, D. Fried, M. Staninec, and C. L. Darling, "Near infrared imaging of teeth at wavelengths between 1200 and 1600 nm," *Proc SPIE,* vol. 7884, p. 78840X, 2011.

[17] L. Karlsson, A. M. A. Maia, B. B. C. Kyotoku, S. Tranæus, A. S. L. Gomes, and W. Margulis, "Near-infrared transillumination of teeth: measurement of a system performance," *J Biomed Opt,* vol. 15, no. 3, pp. 036001-036001-8, 2010.

[18] C. Lee, C. L. Darling, and D. Fried, "In vitro near-infrared imaging of occlusal dental caries using germanium enhanced CMOS camera," *Proc SPIE,* vol. 7549, p. 75490K, 2010.

[19] C. Lee, D. Lee, C. L. Darling, and D. Fried, "Nondestructive assessment of the severity of occlusal caries lesions with near-infrared imaging at 1310 nm," *J Biomed Opt,* vol. 15, no. 4, p. 047011, 2010 2010.

[20] J. C. Simon *et al.*, "Near-IR and CP-OCT imaging of suspected occlusal caries lesions," *Lasers in Surgery and Med,* vol. 49, no. 3, pp. 215-224, 2017.

[21] M. Staninec *et al.*, "Nondestructive Clinical Assessment of Occlusal Caries Lesions using Near-IR Imaging Methods," *Lasers in Surgery and Med,* vol. 43, no. 10, pp. 951-959, 11/22 2011.

[22] H. Tom, J. C. Simon, K. H. Chan, C. L. Darling, and D. Fried, "Near-infrared imaging of demineralization under sealants," *J Biomed Opt,* vol. 19, no. 7, pp. 077003-077003, 2014.

[23] J. Wu and D. Fried, "High Contrast Near-infrared Polarized Reflectance Images of Demineralization on Tooth Buccal and Occlusal Surfaces at λ=1310-nm," *Lasers in Surgery and Med,* vol. 41, no. 3, pp. 208-213, 2009.

[24] D. Fried, R. E. Glena, J. D. B. Featherstone, and W. Seka, "Nature of light scattering in dental enamel and dentin at visible and near-infraredwavelengths," *Applied Optics,* vol. 34, no. 7, pp. 1278-1285, 1995/03/01 1995.

[25] L. Karlsson, "Caries detection methods based on changes in optical properties between healthy and carious tissue," *International Journal of Dentistry,* vol. 2010, no. 270729, 2010.

[26] K. Angelino, D. A. Edlund, and P. Shah, "Near-Infrared Imaging for Detecting Caries and Structural Deformities in Teeth," *IEEE J Transl Eng Health Med,* vol. 5, pp. 1-7, 2017.

[27] G. Li, "Patient radiation dose and protection from cone-beam computed tomography," *Imaging Science in Dentistry,* vol. 43, no. 2, pp. 63-69, 2013.

[28] E. C. Almaz, J. C. Simon, D. Fried, and C. L. Darling, "Influence of stains on lesion contrast in the pits and fissures of tooth occlusal surfaces from 800-1600-nm," *Proc SPIE,* doi: 10.1117/12.2218663 vol. 9692, p. 96920X, Feb. 2016.